2018 IEEE-RAS 18th International Conference on Humanoid Robots (Humanoids)
Beijing, China, November 6-9, 2018

Dynamic Model of Exoskeleton based on Pneumatic Muscle Actuators and Experiment Verification

Yu Cao, Jian Huang*, Zhangbo Huang, Xikai Tu, Hongge Ru, Cheng Chen and Jun Huo

***Abstract*— To assist the elderly people and the patients with neurologic injuries for rehabilitation, the robot-assisted therapy is one of the most remarkable methods for this purpose. In this paper, we developed an exoskeleton based on Pneumatic Muscle Actuators (PMAs). By describing characteristics of human walking, a novel design was proposed to improve the walking comfort of the wearer. In addition, the dynamics of the exoskeleton were analyzed and divided into three parts: the modeling of PMAs, antagonistic configuration of PMAs and the mechanical structure of exoskeletons. The dynamics of the exoskeleton was established according the three parts. Furthermore, a model-free control strategy was utilized to get the exoskeleton properly controlled, which is called Proxy-based Sliding Mode Control. The validity of the exoskeleton model was verified through the comparisons of the simulations and corresponding experiments.**

I. INTRODUCTION

There has been an increasing interest in developing the wearable exoskeleton to assist the elderly people and the patients with neurologic injuries for rehabilitation. Compared with traditional therapies, robot-assisted therapies can save the efforts of medical staff and enhance rehabilitated efficiency [1]. Over the past decade, different prototype exoskeletons have been designed to meet the requirement of clinical applications [2]-[5]. LOKOMAT is the one of the most famous lower limb exoskeletons that is currently available on the market and has been studied in many research laboratories [6]-[7]. It is comprised of a body weight support system, a treadmill and motor powered leg orthosis. Through the three parts of coordinated control, it can effectively assist patients to complete rehabilitation processes. However, human walking is a kind of complex behavior which is the results of interaction among neural signals, human skeletons, and muscles. Hence, gait pattern varies from different people. At present, most of the lower extremity exoskeleton robots are mainly designed to achieve the rotation of the hip, knee, and ankle joints, without considering exoskeleton weight, different human body sizes and floating center of gravity, which may cause discomfort when people wear the lower limb exoskeleton. Besides, such motor-controlled exoskeletons are usually expensive and lack of compliance, which causes difficulties in various fields.

*The work of J. Huang was supported by the National Natural Science Foundation of China under Grant 61473130, the Science Fund for Distinguished Young Scholars of Hubei Province 2015CFA047, and the Beijing Advanced Innovation Center of Intelligent Robots and Systems under Grant 2016IRS10, and the Graduate Innovation and Entrepreneurship Foundation of Huazhong University of Science and Technology under Grant 5003184017.

Y. Cao, J. Huang*, Z. Huang, H. Ru, C. Chen, and J. Huo are with the Key Laboratory of the Ministry of Education for Image Processing and Intelligent Control, School of Automation, Huazhong University of Science and Technology, Wuhan 430074, China. J. Huang is also with the Beijing Advanced Innovation Center of Intelligent Robots and Systems, Beijing 100081, China. Email: cao_yu@hust.edu.cn, huang_jan@mail.hust.edu.cn, huang_zb@hust.edu.cn, ruhongge@hust.edu.cn, hust_cheng@hust.edu.cn, junhuo@hust.edu.cn

X. Tu is with the School of Industrial Design, Hubei University of Technology, Wuhan 430068, China. Email: tuxikai@gmail.com

Fig. 1. The overall composition of the exoskeletal system.

The Pneumatic Muscle Actuator (PMA) is an essentially compliant actuator that has been considered as a novel type of actuation in recent years. Because of its favorable features of high force ratio, no mechanical parts, lightweight, low cost and so on [8], the PMA has become an important choice for rehabilitation robots, especially exoskeletons. In addition, it is safe and suitable for the rehabilitation applications due to their inherent compliance and limited maximum contraction. Tu [9] developed a hip-knee exoskeleton prototype powered by PMAs with Functional Electrical Stimulation, which induced paralyzed muscles to realize ankle joint rehabilitation training. Cao [10] presented a gait exoskeleton driven by the antagonistic configurations of the PMAs with MIMO sliding mode control. But PMAs possess strong nonlinearity, hysteresis and time-varying parameters. Consequently, precisely control of PMAs is a challenging problem. To attain satisfactory control performance, various control strategies have been investigated, including dynamic surface control [11], proportional-integral-derivative (PID) control [12], fuzzy PD+I control [13], active disturbance rejection

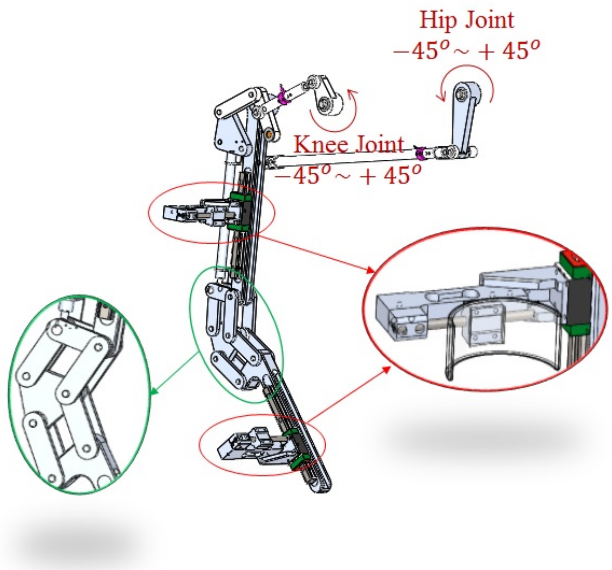

Fig. 2. The mechanical structure of exoskeleton.

control [14], sliding mode control [15], adaptive control [16] and so on. However, the PMAs-driven exoskeleton is often difficult to model, and the dynamics usually contains model uncertainties and external disturbances. A model-free control strategy may meet the requirement of controlling the exoskeleton with complex dynamics. Model-free control strategies like high gain PID control involve some risks of unsafe behaviors in cases of the abnormal event. Therefore, considering the above factors, we would like to propose a lower limb exoskeleton with a novel mechanical structure and a proper control strategy to meet the requirement of comfortable wearing.

In this paper, we developed an exoskeleton based on characteristics of human walking to improve the walking comfort of wearers. Also, the dynamics of the exoskeleton was analyzed for our future investigation. Meanwhile, to get the exoskeleton precisely controlled without sacrificing safety, proxy-based sliding mode control (PSMC) [17] was utilized, which is a novel position control that is as accurate as conventional PID control but is capable of slow, overdamped resuming motion without overshoots from large positional errors. With this method, both simulations and experiments were conducted to verify the effectiveness of the proposed dynamical model for the exoskeleton.

II. Mechanical Design

In order to provide corrective forces or torques to legs of subjects, a lower limb exoskeleton system was developed, as shown in Fig 1. The overall exoskeleton system consists of three parts: a body weight support system, a treadmill and a pair of PMAs-driven exoskeletons. When people are walking on the treadmill, the body weight support system is able to assist people to maintain balance, and the exoskeletons can provide necessary training to the movement of the legs.

The most important portion of this system is the PMAs-driven exoskeletons which directly interact with human legs. The main part includes a hip joint, a thigh, a knee joint, and a lower leg, as shown in Fig 2. Taking into account different body sizes of people, two sliding blocks are designed to fit various people. Also, during the human movement, the rotation center of the knee joint will change, and its instantaneous trajectory is "J" type [18]. Thus, an anthropomorphic design of knee joint is presented to make the wearer comfortable while walking.

On the other hand, the hip joint and knee joint are rotation joints. Since a single PMA can only provide unidirectional actuation, an antagonistic configuration of PMAs is utilized to drive a rotational joint. An exoskeleton has two DoFs, including knee flexion/extension and hip flexion/extension. Hence, two groups of the antagonistic configuration of PMAs are applied to control the exoskeleton.

For the sake of reducing the weight of exoskeleton and alleviating the burden on the human body, we design a support frame for PMAs. Generally, antagonistic PMAs are controlled with respect to

$$\begin{cases} P_a = P_{0a} + \Delta P \\ P_b = P_{0b} - \Delta P \end{cases} \tag{1}$$

Where P_a, P_b are the input pressures of the antagonistic PMAs, respectively. P_{0a}, P_{0b} present the nominal pressures. ΔP denotes the control signal. In this way, one PMA in an antagonistic pair will be inflated and the other one will be deflated, then a rotation torque can be generated. With parallel four-bar transmission, the generated torques can be almost transferred to the hip and knee joints of the exoskeleton. Therefore, PMAs can be separated from the mechanical structure of the powered leg-orthoses, by which the weight of the exoskeleton can be reduced.

III. Dynamics of Exoskeleton

The two PMAs-driven exoskeletons are symmetrical, so only one of them needs to be modeled. From the preceding, its main structure is comprised of two pairs: PMAs and the mechanical structure. Hence, the dynamics of exoskeleton can be formulated as the combination of the mechanical structure and two antagonistic configurations of PMAs that drive the hip joint and knee joint, separately.

A. Modeling of PMA

The generalized three-element model of a PMA is presented as the parallel of a contractile element, a spring element and a damping element [19]. The dynamics can be expressed as:

$$\begin{cases} m\ddot{x} + b(P)\dot{x} + k(P)x = f(P) - mg \\ b_i(P) = b_{i0} + b_{i1}P \quad (inflation) \\ b_d(P) = b_{d0} + b_{d1}P \quad (deflation) \\ k(P) = k_0 + k_1 P \\ f(P) = f_0 + f_1 P \end{cases} \tag{2}$$

where m, x, P are the mass of load, the contractile length of PMA and the air pressure. $b(P), f(P), k(P)$ are respectively, the damping coefficient, the contractile force and the spring

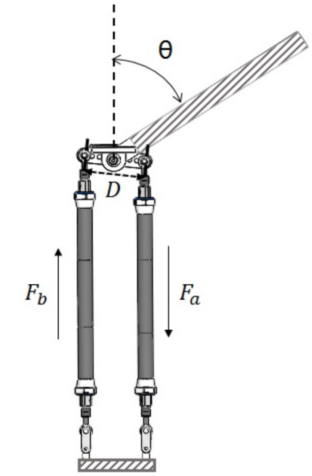

Fig. 3. The antagonistic configuration for one joint.

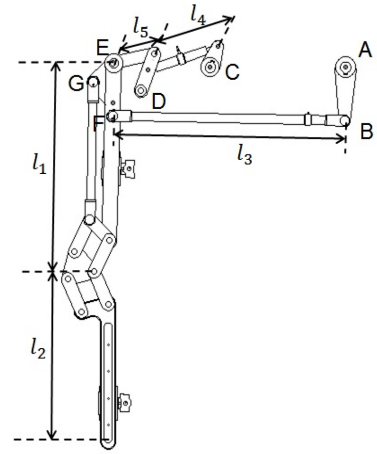

Fig. 4. The exoskeleton structure.

coefficient. These parameters can be determined by following the procedure of [19], [20] with regard to the three-element model. Therefore, the force exerted on the mass m can be described by rewriting (2):

$$F_m = ma = f(P) - b(P)\dot{x} - k(P)x \tag{3}$$

where $a = \ddot{x} + g$ is the acceleration term of the mass.

B. Modeling A Joint

The antagonistic configuration makes a pair of PMAs for one degree of freedom. When one side is contracted, the other side of PMAs contracts to stretch it, as shown in Fig. 3. To simplify analysis, the link that connects two PMAs rotates around the center point and the contraction of PMAs can be expressed as:

$$x_a = r(\frac{\pi}{2} + \theta), x_b = r(\frac{\pi}{2} - \theta) \tag{4}$$

with

$$r = \frac{D}{2}, \theta \in [-\frac{\pi}{2}, \frac{\pi}{2}]$$

where D is the length of the connecting link. θ is the rotation angle. Therefore, based on (3), the torque provided by PMAs can be described as the joint torque which can be expressed as:

$$\tau_a = (f(P_a) - k(P_a)x_a - b_a(P_a)\dot{x}_a)r\,|\sin\theta| \tag{5}$$

$$\tau_b = (f(P_b) - k(P_b)x_b - b_b(P_b)\dot{x}_b)r\,|\sin\theta| \tag{6}$$

where τ_a, τ_b denote the torques of each muscle. x_a, x_b are the contracting lengths. Hence, the torque of a joint can be obtained based on (1)-(6):

$$\begin{aligned} \tau_J &= \tau_a - \tau_b \\ &= [f(P_a) - k(P_a)x_a - b_a(P_a)\dot{x}_a \\ &\quad - f(P_b) + k(P_b)x_b + b_b(P_b)\dot{x}_b]r\,|\sin\theta| \\ &= \tau_0 + \tau_1 \Delta P \end{aligned} \tag{7}$$

with

$$\begin{aligned} \tau_0 &= [P_n f_1 - k_0(x_a - x_b) - k_1(P_{0a}x_a - P_{0b}x_b) \\ &\quad -(b_{0a} + b_{1a}P_{0a})\dot{x}_a + (b_{0b} + b_{1b}P_{0b})\dot{x}_b]r\,|\sin\theta| \\ \tau_1 &= (2f_1 - k_1(x_a + x_b) - b_{1a}\dot{x}_a + b_{1b}\dot{x}_b)r\,|\sin\theta| \\ P_n &= P_{0a} - P_{0b} \end{aligned}$$

C. Driving Principle of Mechanical Structure

In this study, we focus on the dynamics of the mechanical structure, as shown in Fig. 4. The hip joint and knee joint are actuated by two antagonistic configurations of PMAs. Through the four-bar linkage, the joints' driving torque can be effectively transmitted to the hip and knee joints. Two angle encoders are installed on point F, G to obtain the rotation angles of hip and knee joints, respectively. Because of the complex structure, it is difficult to model the exoskeleton accurately. Therefore, we will illustrate the driving principles of the knee and hip joint respectively, to simplify the analysis and obtain the dynamics of the exoskeleton.

To facilitate the presentation, some notations describing parameters of the mechanical structure should be clarified first which are listed as follows:

- l_1 - length of thigh
- l_2 - length of shank
- l_3, l_4, l_5 - length of connecting rods
- A, C, D, E - anchored points
- F, G - angle encoder installation points
- K, I, B, H, M, N - link points

At first, let us focus on the driving torque on the thigh, as shown in Fig. (5b). Four points A, B, E, F are designed to form a parallelogram. Since A, E are anchor points, when a rotational moment τ_h is applied to A, the rod that connects B, F will produce a driving force on the thigh. Then, point E will rotate as point A. To simplify the analysis, we ignore all the friction. Thus, it can be seen as a rotational moment τ_{hip} directly applied to the point E, which drives the thigh. And it satisfies the following relation:

$$\tau_{hip} = \tau_h \tag{8}$$

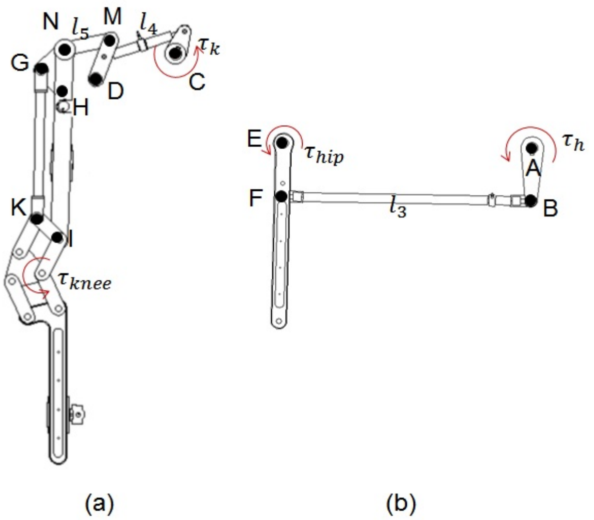

Fig. 5. The actuation of hip and knee joints.

The driving of shank may be a little more complicated, but the driving principle is the same. In Fig. (5a), considering points C, D and rod l_4, a parallelogram is constructed. Then, a rotational moment τ_k' applied to point D will equal to a rotational moment τ_k applied to point C.

$$\tau_k' = \tau_k \tag{9}$$

On the other hand, due to the anthropomorphic structure of knee, the torque that is applied to the knee joint cannot be calculated accurately. Thus, we assume that the torque τ_{knee} applied to the knee joint is equal to the torque τ_{knee}' applied to the point H, on account of the parallel-connected G, H, I, K.

$$\tau'_{knee} = \tau_{knee} \tag{10}$$

Hence, once the relationship between τ_k' and τ_{knee}' is found, the torque applied to the knee joint is determined. Point H is an anchored point to the thigh. In the view of points D, H, M, N, a quadrangle can be figured out. With the rotation of the thigh, the position of point H will alter correspondingly.

Let the distance from point D to rod l_5 be r_1 and the distance from point H to rod l_5 be r_2 and $\alpha = r_1/r_2$. It turns out that

$$\tau_{knee}' = \alpha \tau_k' \tag{11}$$

Finally, we can get the torque applied to the knee joint, which can be expressed as:

$$\tau_{knee} = \alpha \tau_k \tag{12}$$

D. Dynamics of Exoskeleton

The mechanical structure of the exoskeleton is too complex to be accurately modeled. There exist multiple closed chains which make the dynamics of the exoskeleton difficult to be described. But the torque applied to the hip and knee joints can be obtained based on our previous analysis, and the weight of connecting rods and a triangular block are much smaller than that of thigh and shank. Therefore, we simplify the mechanical structure as two-connecting bars, as shown in Fig. 6. Later, the effectiveness of proposed dynamical model will be verified through the comparison study of simulations and corresponding experiments.

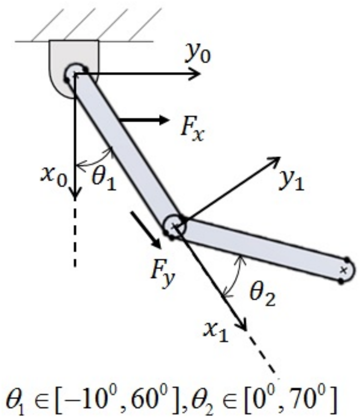

Fig. 6. The simplified model of the exoskeleton.

The dynamics of the system for motion on the sagittal plane can be written in the general Euler-Lagrange form as:

$$\mathbf{M}(\mathbf{q})\ddot{\mathbf{q}} + \mathbf{C}(\mathbf{q}, \dot{\mathbf{q}})\dot{\mathbf{q}} + \mathbf{G}(\mathbf{q}) + \boldsymbol{\tau}_f(\mathbf{q}, \dot{\mathbf{q}}) = \boldsymbol{\tau}_J - \mathbf{J}^T\mathbf{F}$$

where $\mathbf{q} = [\ \theta_1 \quad \theta_2\ ]^T$ is the vector of joint angles and $\mathbf{M}(\mathbf{q})$ is a 2×2 inertia matrix of the exoskeleton leg. $\mathbf{C}(\mathbf{q}, \dot{\mathbf{q}})$ is a centripetal and Coriolis matrix. $\mathbf{G}(\mathbf{q})$ is a 2×1 vector of gravitational torque. $\boldsymbol{\tau}_f(\mathbf{q}, \dot{\mathbf{q}})$ is a vector of frictional force. $\boldsymbol{\tau}_J$ is a 2×1 vector of provided torque by the antagonistic configuration of PMAs. $\mathbf{F}$ is the 2×1 vector of reaction forces with cartesian coordinates: F_x and F_y (Fig. 6), since the rotations of hip and knee joints come from the force F_x, F_y; and $\mathbf{J}$ is the Jacobian matrix.

In consideration of the dynamics of antagonistic PMAs and neglect of friction, the overall dynamics of the exoskeleton can be expressed as:

$$\mathbf{M}(\mathbf{q})\ddot{\mathbf{q}} + \mathbf{N}(\mathbf{q}, \dot{\mathbf{q}}) = \boldsymbol{\tau}_0 + \mathbf{G}\Delta\mathbf{P} \tag{13}$$

where $\mathbf{N}(\mathbf{q}, \dot{\mathbf{q}})$ is the sum of $\mathbf{C}(\mathbf{q}, \dot{\mathbf{q}})\dot{\mathbf{q}}$ and $\mathbf{G}(\mathbf{q})$. Taking (7) as the input torque and combining (8), (12), we can get

$$\begin{array}{c} \boldsymbol{\tau}_0 = [\ \tau_{h0} \quad \alpha\tau_{k0}\ ]^T \\ \Delta\mathbf{P} = [\ \Delta P_{hn} \quad \Delta P_{kn}\ ]^T \end{array} \quad \mathbf{G} = \begin{bmatrix} \tau_{h1} & 0 \\ 0 & \alpha\tau_{k1} \end{bmatrix}$$

$\tau_{h0}, \tau_{k0}, \tau_{h1}, \tau_{k1}$ are the input torques of hip and knee joint produced by antagonistic configurations of PMAs. $\Delta P_{hn}, \Delta P_{kn}$ are the control signals of the hip and knee joints, respectively. The inertia matrix can be denoted as follows:

$$\mathbf{M}(\mathbf{q}) = \begin{bmatrix} k_1 + k_2 + m_2 a_1^2 + m_1 l_1^2 + I_1 & k_1 + k_2 \\ k_1 + k_2 & k_1 \end{bmatrix}$$

$$\mathbf{N}(\mathbf{q}, \dot{\mathbf{q}}) = \begin{bmatrix} \Delta_1 \\ \Delta_2 \end{bmatrix}$$

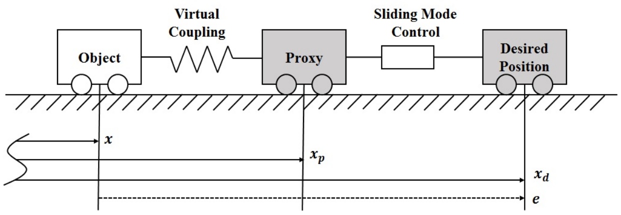

Fig. 7. The principle of PSMC.

with

$$k_1 = m_2 l_2^2 + I_2, k_2 = m_2 a_1 l_2 cos(\theta_2)$$

$$\Delta_1 = -m_2 a_1 l_2 sin(\theta_2)\dot{\theta}_2^2 - 2m_2 a_1 l_2 sin(\theta_2)\dot{\theta}_2\dot{\theta}_1$$
$$+m_2 g a_1 cos(\theta_1) + m_2 g l_2 cos(\theta_1+\theta_2) + m_1 g l_1 cos(\theta_1)$$
$$\Delta_2 = m_2 a_1 l_2 sin(\theta_2)\dot{\theta}_1^2 + m_2 g l_2 cos(\theta_1+\theta_2)$$

where m_1, m_2 are weights of thigh and shank; a_1, a_2 are the lower limb lengths; l_1, l_2 are the GOFs to the coordinate origin. I_1, I_2 are the moments of inertia, respectively.

IV. CONTROL DEVELOPMENT

The exoskeleton possesses features of strong nonlinearity, time-varying parameters and uncertainties. Although the dynamics has been proposed, it is difficult to model these uncertainties. Consequently, Proxy-based Sliding Mode Control (PSMC) is applied to obtain favorable control performance for the system. PSMC is a novel position control that is as accurate as conventional PID control but is capable of slow, overdamped resuming motion without overshoots from large positional errors. By transforming signum function to unit saturation function, it is able to reduce the chattering phenomenon effectively.

The principle of PSMC is shown in Fig. 7. The object is connected to a virtual object, which is called a "proxy", by means of a PID-type virtual coupling. The PID controller causes an interaction force F_{pid}. While the proxy is controlled by an SMC that produces a force F_{SMC} to make the proxy track the desired trajectory.

The SMC law that is applied to the proxy is given by:

$$f_{SMC} = F\text{sgn}(\sigma_1) \tag{14}$$

with

$$\sigma_1 = x_d - x_p + \lambda(\dot{x}_d - \dot{x}_p)$$

where x, x_d, x_p are the object's position, desired trajectory and proxy's position, respectively. λ, F are positive constants. Let

$$a = \int_0^t (x_p - x)dt$$

then PID controller provides the force can be expressed as:

$$f_{PID} = k_p\dot{a} + k_i a + k_d\ddot{a} \tag{15}$$

Let another sliding surface

$$\sigma = x_d - x + \lambda(\dot{x}_d - \dot{x})$$

TABLE I
THE PARAMETERS OF THE PMAS AND EXOSKELETON.

Parameter	Value(Unit)	Parameter	Value(Unit)
$f_0(\times 10^2)$	7.2 (N)	$f_1(\times 10^0)$	5.6(N/bar)
$k_{01}(\times 10^4)$	2.28 (N/m)	$k_{11}(\times 10^{-1})$	1.23(N/(m.bar))
$b_{0i}(\times 10^3)$	4.04 (N.s/m)	$b_{1i}(\times 10^{-2})$	2.8(N.s/(m.bar))
$b_{0d}(\times 10^3)$	2.4 (N.s/m)	$b_{1d}(\times 10^{-2})$	1.0(N.s/(m.bar))
$r(\times 10^{-2})$	7.5 (N.s/m)	$g(\times 10^0)$	9.8(m/s)
$m_1(\times 10^0)$	2.0 (kg)	$m_2(\times 10^1)$	2.3 (kg)
$a_1(\times 10^{-1})$	4.8 (m)	$a_2(\times 10^{-1})$	3.9 (m)
$I_1(\times 10^{-1})$	4.11 (kg.m^2)	$I_2(\times 10^{-1})$	2.50 (kg.m^2)

Considering the proxy, the equation of motion can be governed by:

$$m_p\ddot{x}_p = f_{SMC} - f_{PID} \tag{16}$$

where m_p is mass of the proxy.

Setting m_p equals to zero, then $f_{SMC} = f_{PID} \equiv f$ is satisfied. Due to the relation of signum function and the saturation function [17], the control law of PSMC can be obtained as:

$$f = Fsat(\frac{k_d}{F}(\frac{\sigma - \dot{a}}{\lambda} + \frac{k_p\dot{a} + k_i a}{k_d})) \tag{17}$$

with

$$sat(y) = \begin{cases} \text{sgn}(y), if|y| > 1 \\ y, \quad\quad if|y| \leq 1 \end{cases}$$

V. SIMULATION AND EXPERIMENT STUDIES

To verify the correctness of our proposed dynamics, some simulations and corresponding experiments are performed on the exoskeleton. In all the simulations, parameters of the PMAs and exoskeleton were identified offline, as shown in Table I.

Both experiments and simulations were conducted. In the experiment, PSMC control strategy was firstly utilized to get the physical exoskeleton properly controlled with sinusoidal functions. The generated control signals were then inputted into the model of exoskeleton in the simulation to verify whether the behaviors of the model are similar to the physical exoskeleton based on hip and knee joint angles.

The results are shown in Fig. 8. The first line of pictures denote the control signals of the hip and knee joints based on PSMC. In the first 5 second, there were no control signals because we set the system to start after 5 seconds. The sampling time is $T_s = 0.0005s$. The control signals were acquired directly from the controller instead of the actual signal fed back by the valve. This pressure signal may not be accurate, but it is suitable for our simulations.

For the second line, the tracking performances of the hip and knee joints are expressed. It is shown that the PSMC can effectively control the exoskeleton. This model-free control strategy brings convenient for the complex dynamics of objects. However, there exist tracking errors in this experiment even after good adjustment for parameters.

For the third line, comparisons between the simulated joint angles and the real joint angles are presented. With the same control signals, the behavior of the simulated hip joint angle is similar to the real situation. There is only a difference

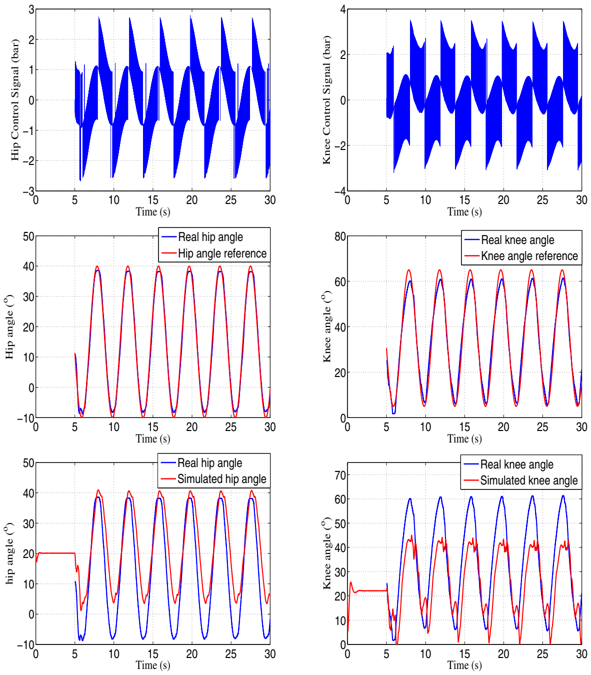

Fig. 8. From left to right, the figures are the control signals of hip and knee joints; control performance of the hip and knee joint based on PSMC; the comparisons between the simulated joint angles and the real joint angles.

in the magnitude of the amplitude. This is reasonable since the parameters of the PMAs can not be accurately identified, owing to the measurement errors, nonlinearities and uncertainties. On the other hand, the simulated knee joint seems a phase difference from the real one. There are two reasons for this phenomenon. Firstly, referring to (12), α is a time-varying parameter instead of certain value. It is difficult to be calculated. Thus, we assume it as a cosine function greater than 0. Secondly, when we concern the moment of the knee joint, there may be a certain offset that we have not taken into account.

These inaccurate parts can be seen as disturbance of the system that can be compensated in the model-based control strategies. We will investigate them in our future work.

VI. Conclusion

Robot-assisted therapies can increase the intensity of training, save the efforts of medical staff and enhance rehabilitated efficiency, which largely improves the rehabilitation process for the patients with neurologic injuries. Therefore, we developed a exoskeleton based on characteristics of human walking. It was comprised of treadmill, body weight support system, and the mechanical structure. The dynamics of the exoskeleton was analyzed, and a model-free control strategy called proxy-based sliding mode control was utilized to get the exoskeleton properly controlled. The effectiveness of proposed dynamical model was verified through the comparison study of simulations and corresponding experiments.

In our future work, we would like to propose model-based control strategies to compensate the inaccurate model of the exoskeleton, with which the exoskeleton can be precisely controlled.

References

[1] S. H. Chen et al., ”Assistive Control System for Upper Limb Rehabilitation Robot,” in IEEE Transactions on Neural Systems and Rehabilitation Engineering, vol. 24, no. 11, pp. 1199-1209, Nov. 2016.

[2] Stanley Fisher, Leah Lucas & T. Adam Thrasher, ”Robot-Assisted Gait Training for Patients with Hemiparesis Due to Stroke” in Topics in Stroke Rehabilitation, Vol. 18, Issue 3, 2011.

[3] S. K. Banala, S. K. Agrawal, S. H. Kim and J. P. Scholz, ”Novel Gait Adaptation and Neuromotor Training Results Using an Active Leg Exoskeleton,” in IEEE/ASME Transactions on Mechatronics, vol. 15, no. 2, pp. 216-225, April 2010.

[4] H. Vallery, J. Veneman, E. van Asseldonk, R. Ekkelenkamp, M. Buss and H. van Der Kooij, ”Compliant actuation of rehabilitation robots,” in IEEE Robotics & Automation Magazine, vol. 15, no. 3, pp. 60-69, September 2008.

[5] S. K. Banala, S. H. Kim, S. K. Agrawal and J. P. Scholz, ”Robot Assisted Gait Training With Active Leg Exoskeleton (ALEX),” in IEEE Transactions on Neural Systems and Rehabilitation Engineering, vol. 17, no. 1, pp. 2-8, Feb. 2009.

[6] Colombo, G, M. Wirz, and V. Dietz, ”Driven gait orthosis for improvement of locomotor training in paraplegic patients.” in Spinal Cord, vol. 39, pp. 252-255, Jun. 2001.

[7] S. Jezernik, G. Colombo and M. Morari, ”Automatic gait-pattern adaptation algorithms for rehabilitation with a 4-DOF robotic orthosis,” in IEEE Transactions on Robotics and Automation, vol. 20, no. 3, pp. 574-582, Jun. 2004.

[8] Dzahir, A. M. and S.-i. Yamamoto, ”Recent Trends in Lower-Limb Robotic Rehabilitation Orthosis: Control Scheme and Strategy for Pneumatic Muscle Actuated Gait Trainers,”, in *Robotics*, vol. 3, no. 2, pp. 120-148, Mar. 2014.

[9] X. Tu, J. Huang and J. He, ”Leg hybrid rehabilitation based on hip-knee exoskeleton and ankle motion induced by FES,” 2016 International Conference on Advanced Robotics and Mechatronics (ICARM), Macau, 2016, pp. 237-242.

[10] J. Cao, S. Q. Xie and R. Das, ”MIMO Sliding Mode Controller for Gait Exoskeleton Driven by Pneumatic Muscles,” in IEEE Transactions on Control Systems Technology, vol. 26, no. 1, pp. 274-281, Jan. 2018.

[11] J. Wu, J. Huang, Y. Wang and K. Xing, ”Nonlinear Disturbance Observer-Based Dynamic Surface Control for Trajectory Tracking of Pneumatic Muscle System,” in IEEE Transactions on Control Systems Technology, vol. 22, no. 2, pp. 440-455, March 2014.

[12] G. Andrikopoulos, G. Nikolakopoulos and S. Manesis, ”Advanced Nonlinear PID-Based Antagonistic Control for Pneumatic Muscle Actuators,” in IEEE Transactions on Industrial Electronics, vol. 61, no. 12, pp. 6926-6937, Dec. 2014.

[13] S. W. Chan, J. H. Lilly, D. W. Repperger and J. E. Berlin, ”Fuzzy PD+I learning control for a pneumatic muscle,” Fuzzy Systems, 2003. FUZZ '03. The 12th IEEE International Conference on, 2003, pp. 278-283 vol.1.

[14] Hongjiu Yang, Yang Yu, Jinhui Zhang, Angle tracking of a pneumatic muscle actuator mechanism under varying load conditions, Control Engineering Practice, vol. 61, pp 1-10, 2017.

[15] J. H. Lilly and Liang Yang, ”Sliding mode tracking for pneumatic muscle actuators in opposing pair configuration,” in IEEE Transactions on Control Systems Technology, vol. 13, no. 4, pp. 550-558, July 2005.

[16] L. Zhu, X. Shi, Z. Chen, H. T. Zhang and C. H. Xiong, ”Adaptive Servomechanism of Pneumatic Muscle Actuators With Uncertainties,” in IEEE Transactions on Industrial Electronics, vol. 64, no. 4, pp. 3329-3337, April 2017

[17] R. Kikuuwe, S. Yasukouchi, H. Fujimoto and M. Yamamoto, ”Proxy-Based Sliding Mode Control: A Safer Extension of PID Position Control,” in IEEE Transactions on Robotics, vol. 26, no. 4, pp. 670-683, Aug. 2010.

[18] James W, stuart H. Technical note: beyond the four-bar knee. Journal of prosthetics and orthotics,vol. 10, no. 3, pp. 77 -80, 1998

[19] D. B. Reynolds, D. W. Repperger, C. A. Phillips, and G. Bandry, ”Modeling the Dynamic Characteristics of Pneumatic Muscle,” in *Annals of Biomedical Engineering*, vol. 31, pp. 310-317, Mar. 2003.

[20] Yong Mao, Jiaxin Wang, Shi Li and Zhuo Han, ”Energy-Efficient Control of Pneumatic Muscle Actuated Biped Robot Joints,” 2006 6th World Congress on Intelligent Control and Automation, Dalian, 2006, pp. 8881-8885.